CHINESE JOURNAL OF GEOPHYSICS Vol.50, No.5, 2007, pp: 1300∼1308

THE 1992 LANDERS EARTHQUAKE: EFFECT OF CRUSTAL HETEROGENEITY ON EARTHQUAKE GENERATION

TIAN You[1,2] ZHAO Da-Peng[2] SUN Rou-Mei[1] TENG Ji-Wen[1,3]

1 *Institute of Geology and Geophysics, Chinese Academy of Sciences, Beijing* 100029, *China*

2 *Research Center for Prediction of Earthquakes and Volcanic Eruptions, Tohoku University, Sendai* 980-8578, *Japan*

3 *Jilin University, Changchun* 130026, *China*

Abstract In order to understand the relationship between earthquake occurrence and crustal heterogeneities, we used 107401 P- and 19624 S-wave high-quality arrival times from the 1992 Landers aftershocks and other local earthquakes which were recorded by both permanent and temporary stations in Southern California to determine detailed three-dimensional P- and S-wave velocity and Poisson's ratio structures beneath the Landers earthquake area. Our results show a correlation between the seismic rupture zones and crustal heterogeneities. The distribution of the Landers aftershocks is cluster-like and separated or terminated in the area where low-velocity anomalies exist. Most of the large earthquakes with magnitudes bigger than 4 occur in or around areas with high P-wave velocity. The possibility is that high-velocity areas are probably brittle and strong parts which can sustain seismogenic stress, and so can generate earthquakes. In contrast, low-velocity areas may have either higher degree of fracture, high fluid pressure, or higher temperatures where deformation is more likely to be aseismic. In addition, we infer that fluids exist in the Landers earthquake area from the distribution of P- and S-wave velocity and Poisson's ratio. The existence of fluids may weaken the surrounding crustal rocks, then trigger strong earthquakes.

Key words Southern California, Landers earthquake, Seismic tomography, Poisson's ratio, Fluids

1 INTRODUCTION

Southern California is seismically one of the most active areas in the world and has been paid much attention to by many seismologists. This region has a very complex geological structure and active seismicity. The primary active fault, San Andreas Fault, stretches over 1200 km and runs through the entire California, which has become a boundary to separate the Pacific and the American plates[1] (Fig. 1).

It is well known that earthquake disaster is one of the largest natural disasters, and it could bring enormous harm to mankind and the development of society[2]. On June 28, 1992, a magnitude (M_w) 7.3 earthquake occurred in Landers, South California in USA. The epicenter is located at southeastern Mojave Desert, approximately 180 km east of Los Angeles (Fig. 1). The damage of the earthquake was very large. It caused a surface rupture extending over a distance of more than 70 km. Near the epicenter, the surface displacement of the fault trace was approximately 3 meters; near the northern end of the fault, the displacement reached 6.7 meters[3]. After the Landers

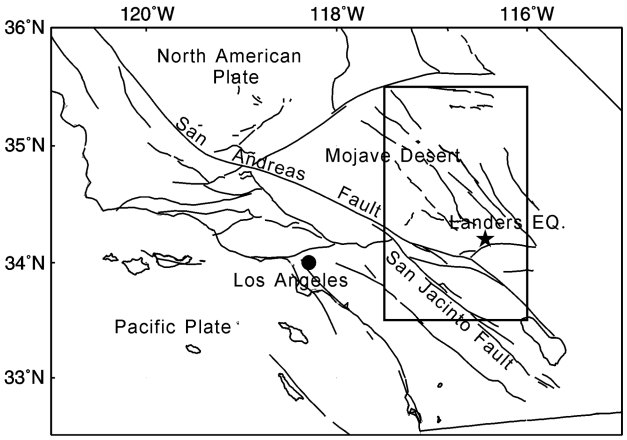

Fig. 1 Tectonic background of Southern California
The box shows the present study area, the star symbol represents the epicenter of the Landers mainshock. Major faults are shown by solid lines.

E-mail: you_tian918@yahoo.coms

mainshock, over 10000 aftershocks were recorded in the following several months.

The present study area, which is shown by a rectangle in Fig. 1, is located in the west and middle Southern California. The San Andreas Fault and San Jacinto Fault run through this region. The area contains several geological domains, such as eastern part of Transverse Ranges, Eastern California Shear zone, Salton Trough and so on. Zhao and Kanamori[4] used seismic tomography to study the crustal structure and seismicity of this region, but because of limited data set available then, they only used P-wave arrival times which were only recorded by permanent stations. Although the present study area is the same as that of Zhao and Kanamori (1993), we collected many P-wave arrival times recorded by temporary stations so that seismic rays crisscross well in the study area. In addition, we inverted for S-wave velocity and Poisson's ratio (σ) structure. We discuss the deep structure and tectonic environment for the preparation and occurrence of local earthquakes in Landers, then try to clarify the relationship between earthquake occurrence and crustal heterogeneities. Investigation of the detailed crustal structure in and around the source area may provide crucial information for understanding the earthquake physics.

2 DATA

P- and S-wave arrival times used in the present study were recorded by Southern California Seismic Network of the US. We selected 1445 events from aftershocks which were recorded by both permanent and temporary stations (Fig. 2b). In order to obtain better inversion results, we also collected 1418 local events occurred during the period from 1981 to 1994 to improve the event distributtion. Most of the events have more than 20 P arrivals. Fig. 3 shows the epicenter distribution of 2863 local events, which are well distributed in the entire study area.

In order to avoid the influence of heterogeneities out of the study area, we only used the arrival times with epicentral distance less than 190 km. Finally, the total number of first P- and S-wave arrival times is 107401 and 19624, respectively. The picking accuracy of P-wave arrival times is less than 0.1 s, and the accuracy of S-wave arrival times is about 0.15 s.

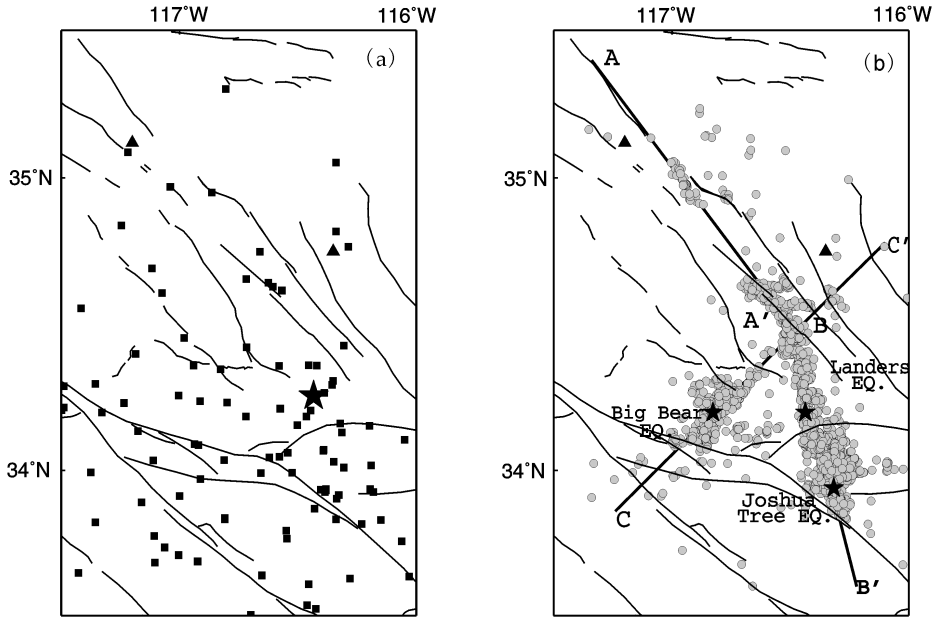

Fig. 2 Distribution of the seismic stations (a) and epicentral distribution of the Landers aftershocks which occurred from June 28 to August 31, 1992 and locations of the three vertical cross sections (b) The solid triangles denote the volcanoes. The star symbols denote mainshock epicenters of the Landers (a) and Landers, Big Bear and Joshua Tree earthquakes (b), respectively.

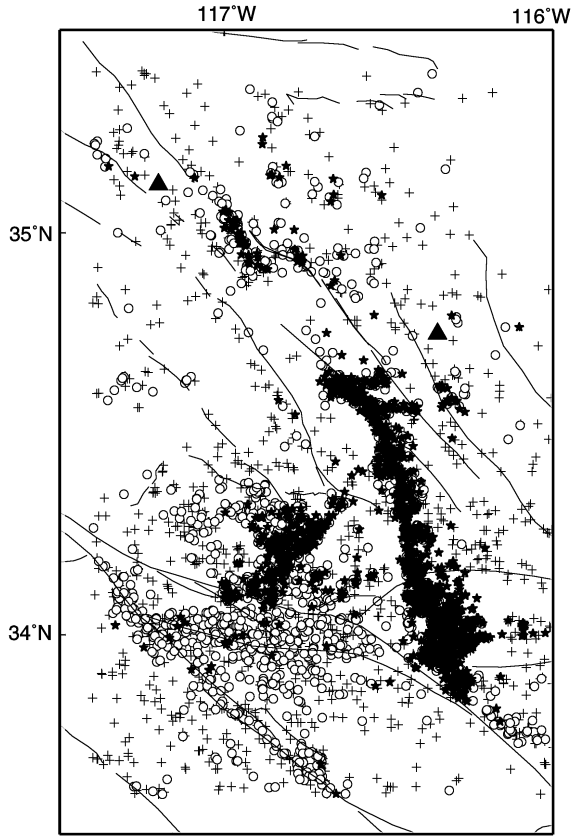

Fig. 3 Epicentral distribution of the earthquakes used in this study

Cross symbols denote the earthquakes which occurred in the period from 1981 to 1992, circles represent the earthquakes occurred from 1993 to 1994, and the star symbols denote the aftershocks of the 1992 Landers earthquake.

3 METHOD

3.1 Seismic Tomography

In recent years, seismic tomography has become one of the most important methods for studying the structure of the earth's interior. Many researchers have obtained significant results by using different tomographic methods[5~9]. In this study, we used the tomographic method of Zhao et al.[10,11]. This method is adaptable to a velocity structure which includes several complex-shaped velocity discontinuities and allows three-dimensional (3-D) velocity variations everywhere in the model. To calculate travel times and ray paths accurately and rapidly, an efficient 3-D ray-tracing technique[10,12] is employed. In order to improve the image solution, arrival times of reflected and converted waves at the discontinuities in the model can be used in the inversion in addition to first P- and S-wave arrival times. The LSQR algorithm[13] with damping and smoothing regularization is used to solve the large and sparse system of observation equations.

3.2 Poisson's Ratio

Poisson's ratio is a key parameter in studying petrologic properties of crustal rocks[14]. From the formula of Poisson's ratio, we can see that it can be determined from P- and S-wave velocities.

$$\sigma = \frac{1}{2}\left(1 - \frac{1}{(V_{\rm P}/V_{\rm S})^2 - 1}\right),$$

where $V_{\rm P}, V_{\rm S}$ and σ denote P-wave velocity, S-wave velocity and Poisson's ratio, respectively. Following this formula, we use the P- and S-wave velocities which are obtained by tomographic inversion to calculate Poisson's ratio. Reliability of Poisson's ratio can be analyzed by P- and S-wave inversion resolution. Using of the information of Poisson's ratio is better than using P- and S-wave velocities alone in identifying the composition of the earth materials. The studies so far showed that the information of Poisson's ratio is very effective in studying the seismicity, especially in finding whether fluids exist in the crustal tectonic environment on the preparation and occurrence of earthquakes[15~17].

4 INVERSION AND RESOLUTION

Whereas the inversion result is not unique, the resolution analysis is very important in seismic tomography. Because the LSQR algorithm can not obtain the resolution matrix directly, researchers often use some methods to estimate resolution. Conducting synthetic tests is an effective method for testing the reliability of tomographic image and its resolution[11,18]. The aim of this method is to estimate that with the data set and grid setting how large velocity anomalies can be revealed, this is decided by the crisscross condition of the rays in the study area. To confirm the main features of the tomographic result, we conducted a synthetic test in the Landers earthquake region. In the area of Landers earthquake epicenter, we put a high-velocity anomaly up to 3% in

the synthetic model (Fig. 4a), then with this initial model, we calculated arrival time residuals using the same stations, events and ray paths as those in the real data set, and usied these data to conduct the inversion. Fig. 4b and Fig. 4c show the final results of this synthetic test. We can see that the high-velocity anomalies are well recovered with little smearing. From the synthetic test, we can see that the tomographic resolution is about 5∼10 km in epicenter area. Because most of the earthquakes occurred in the upper crust, the resolution of the lower crust is much lower, so we primarily discuss the upper crust velocity structure in the present study.

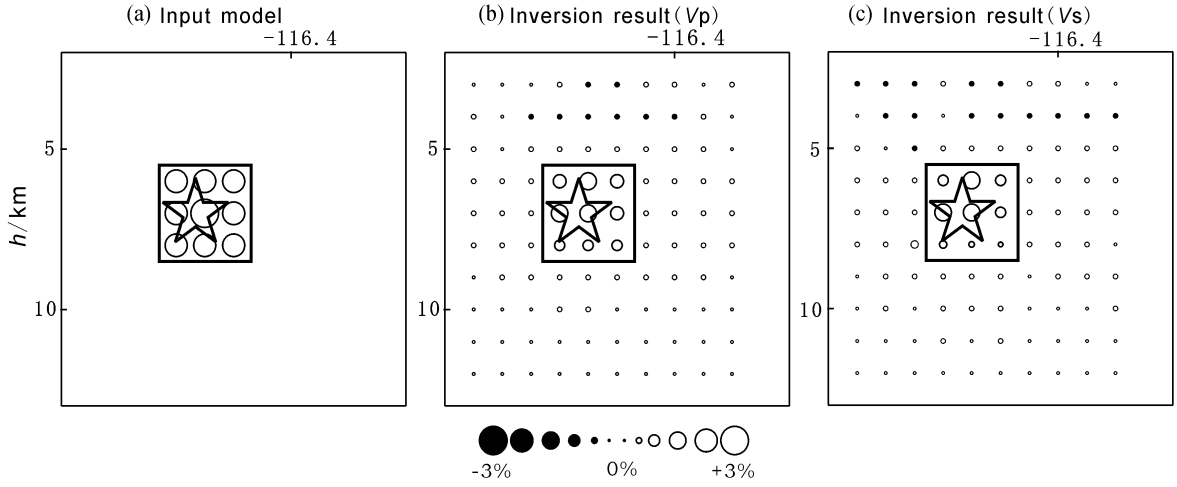

Fig. 4 Results of synthetic test

The left figure shows the input model. The right two figures show the P- and S-wave inversion results of synthetic tests in the Landers source area.

Model parameterization and grid spacing control the tomographic results obtained by inversion, and then influence the discussion on the structure of the earth interior and petrologic properties. Model parameterization is also one of the primary differences among the tomographic methods[19]. In our study, we set up a series of grids, and the velocity perturbation on the grid nodes is taken as the unknown parameters. We conducted many inversions by using different grid spacings, and we found that there is high resolution in the aftershock region. In order to study the fine 3-D velocity structure in the epicenter area, we set up the grid spacing of 5 km in horizontal direction in the final inversion. In the vertical direction (0∼30 km), we set up 10 layers, and the grid spacing is 3 to 5 km.

In inversion, the velocity images are determined at the grids with hit counts (number of rays passing through each grid node) greater than 15. In the present study, over 95% of nodes have more than 15 hit counts for P wave, and at most nodes, the hit counts are more than 100. Because the number of S-wave arrival times is less, we inverted for the velocity perturbation at the nodes with hit counts greater than 10. We have conducted many inversions using different values of damping parameter. We found that the best values of damping parameter for both P and S inversions are 5.0 considering the balance between the reduction of travel time residuals and the smoothness of the 3-D velocity model obtained[20] (Fig. 5).

The starting one-dimensional (1-D) velocity model and Poisson's ratio model for present study area are derived from the crustal model of Kanamori and Hadley[21] in 1975 (Fig. 6). This velocity model is also used to relocate the earthquakes in Southern California Seismic Network.

5 RESULTS AND DISCUSSION

From the synthetic test, the grid spacing of the present study can resolve the velocity anomalies well in the aftershock area. We made three cross sections of velocity (V_P and V_S) and Poisson's ratio (σ) perturbations along the profile shown in Fig. 2b (Figs. 7∼9). Next, we discuss the main features of velocity anomalies in detail.

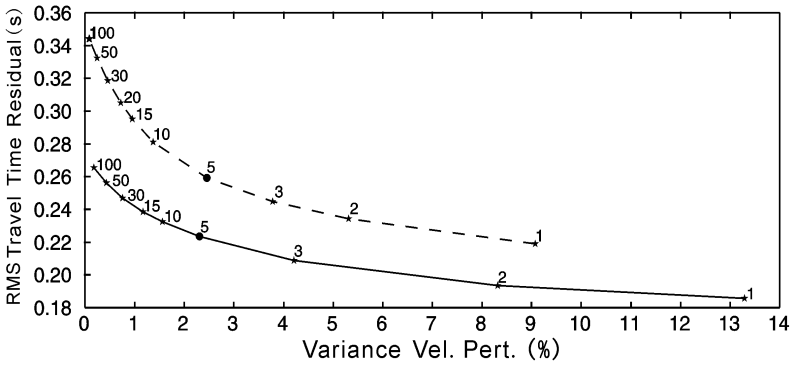

Fig. 5 Trade-off curve for the norm of velocity perturbations in % (horizontal axis) and root-mean-square travel time residuals in second (vertical axis) for P (solid line) and S wave (dash line), respectively

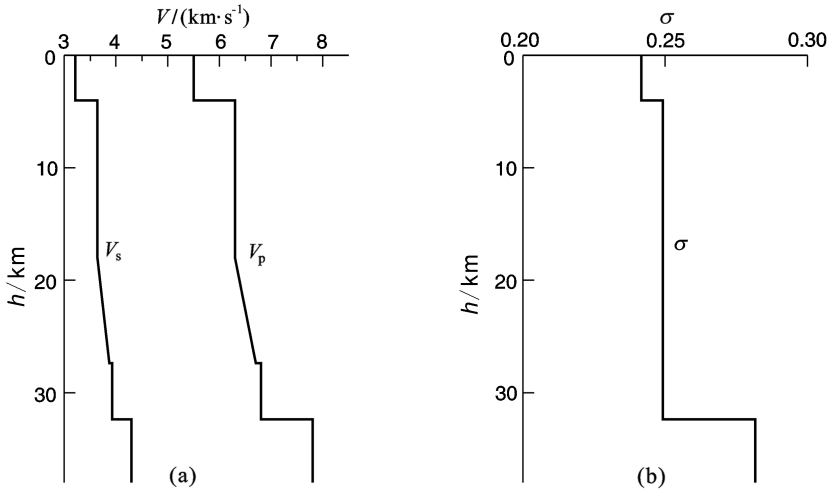

Fig. 6 The initial 1-D P- and S-wave velocity models (a) and Poisson's ratio model (b) in the present study area

The result along the northern segment of the fault zone of the Landers earthquake is shown in Fig. 7. From the P- and S-wave velocity anomaly images, we can see that a prominent low-velocity anomaly exists under the Black Mountain volcano, and it extends to about 10 km depth. From the Poisson's ratio image (σ), a low Poisson's ratio anomaly exists there. In the P-wave velocity image (V_{P}), the two groups of aftershocks are separated by a prominent low-velocity zone which extends to about 10 km depth. The similar result is shown in the S-wave velocity anomaly image (V_{S}) but less visible than P-wave image.

Figure 8 shows the depth distribution of the aftershocks which occurred in the southern segment of the Landers earthquake fault zone and the velocity distribution. The seismicity is terminated near the San Andreas Fault where a low-velocity anomaly exists. In and around the aftershocks, the P- and S-wave velocity structures are more complex. The focal depth of Landers earthquake (M_{w} 7.3) mainshock hypocenter and Joshua Tree earthquake (M_{w} 6.2) which occurred on April 23, 1992 are 7.0 km and 15.2 km depths[4], respectively, a little deeper than the depths of 1 km and 14.2 km determined by SCSN with a 1-D velocity model. The hypocenter of the Landers earthquake is located in a boundary zone where both velocity and Poisson's ratio change drastically and leans to high Poisson's ratio, and a large low P-wave velocity anomaly is visible under the source zone (Fig. 8). The hypocenter of Joshua Tree earthquake which can be considered as a foreshock of the Landers earthquake[3] is located in a large high-velocity and high Poisson's ratio area. The San Andrea fault is just located at the south boundary of the aftershock zone. The distribution characters of aftershocks may indicate that the rupture plane of the fault dips to northeast.

The profile CC′ passes through the Big Bear earthquake and its aftershock area (Fig. 9). The fault rupture of Big Bear earthquake is terminated near the western part of San Andreas Fault, and both San Jacinto fault

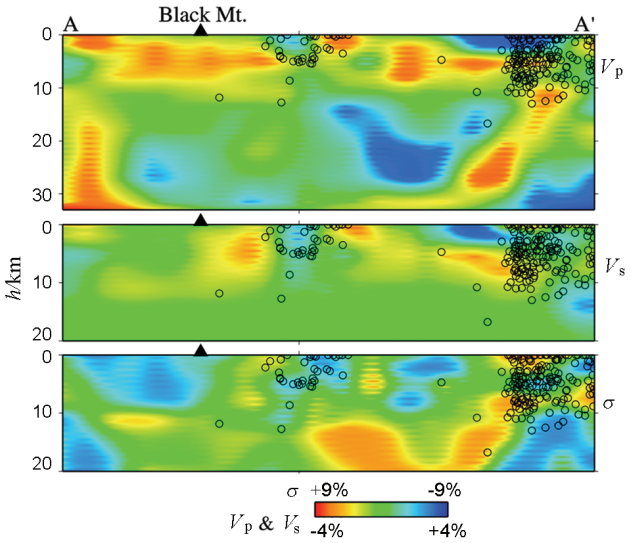

Fig. 7 Tomographic images of P- and S-wave velocity and Poisson's ratio along the profile AA′ which is shown in Fig. 2b

The solid triangle denotes the Black Mountain volcanic center. The circles denote the Landers aftershocks within 5 km along the profile. The velocity perturbation and Poisson's ratio scales (in %) are shown at the bottom.

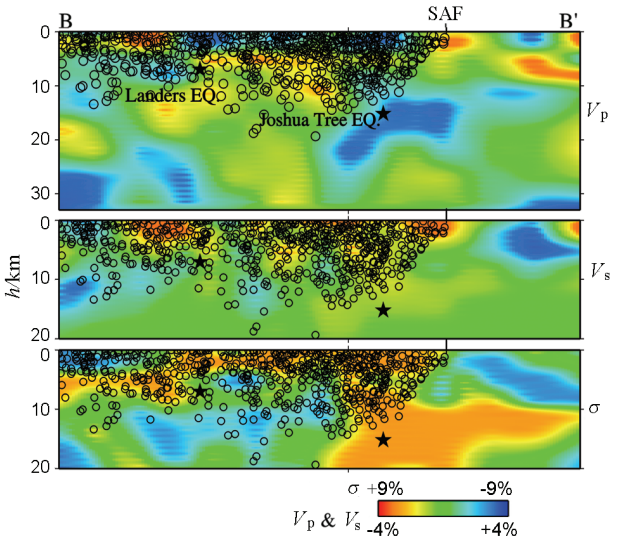

Fig. 8 The same as Fig. 7 but along profile BB′

The star symbols denote the mainshock hypocenters of the Landers earthquake and the Joshua Tree earthquake.

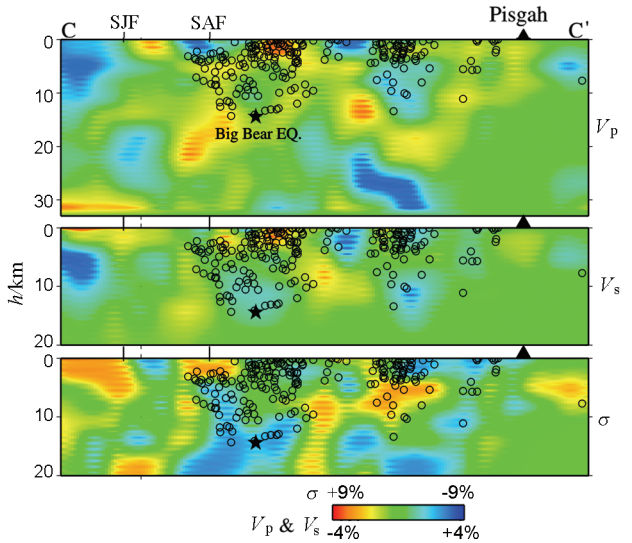

Fig. 9 The same as Fig. 7 but along profile CC′

The solid triangle denotes the Pisgah volcanic center. The star symbol denotes the mainshock hypocenter of the Big Bear earthquake.

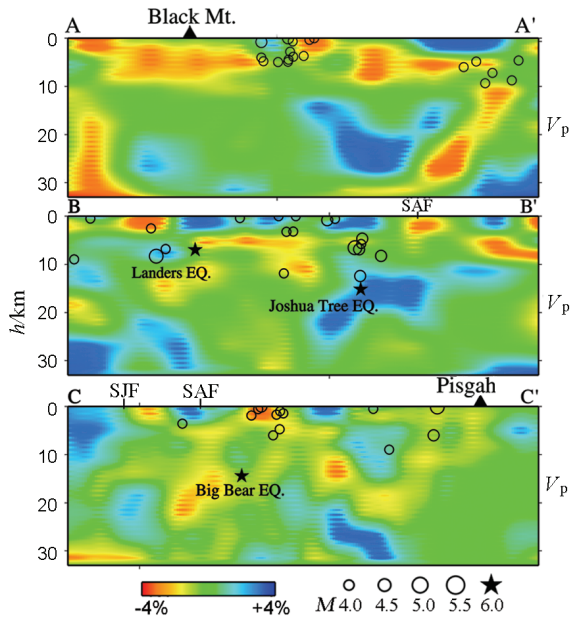

Fig. 10 P-wave velocity images along the profiles of AA′, BB′ and CC′, and distribution of the hypocenters of earthquakes with magnitudes larger than 4.0

The locations of three profiles are shown in Fig. 2b. The velocity perturbation and magnitude scales are shown at the bottom.

and San Andreas Fault are located at the boundary of low-velocity and high-velocity zone. There is a small gap existing in the middle of aftershock region, and in this region, the P- and S-wave velocity are high from 0 to 4 km depth and become low in the deeper area. The Big Bear earthquake is located at 14.4 km depth with a 3-D velocity model[4], slightly deeper than the depth with 1-D velocity model. The hypocenter of Big Bear earthquake is located at the boundary between high-velocity and low-velocity area and in the low Poisson's ratio area. A low P-wave velocity, low S-wave velocity and low Poisson's ratio anomaly is visible below the

Pisgah volcano.

P-wave velocity changes are visible across San Andreas Fault and San Jacinto Fault (Fig. 9).

Both low P-wave and low S-wave velocity exist in the termination region of aftershocks, and previous studies have obtained similar results[22,23]. From the profiles of AA′ and CC′, we can see that the aftershocks are divided into two groups. In order to further study the relationship between earthquake occurrence and velocity structure, we show the P-wave images together with earthquakes within 5 km from the profiles and with magnitudes larger than 4.0 (Fig. 10). We can see clearly that most of these earthquakes are located at the boundary between the low-velocity and high-velocity anomalies or close to the high-velocity zones, and the similar results are obtained by previous studies[24∼28]. The possibility is that high-velocity areas are probably brittle and strong parts which can sustain seismogenic stress, and so can generate earthquakes. In contrast, low-velocity areas may have either higher degree of fracture, high fluid pressure, or higher temperatures where deformation is more likely to be aseismic[4,22].

In recent years, more and more seismologists have paid attention to the effect of crustal fluids[16,17,29∼31]. These studies proved that fluids exist in the crust and upper mantle widely[32]. The hypocenter of the Kobe earthquake occurred in 1995 is located in low P-wave, low S-wave velocity and high Poisson's ratio zone[15], and they explained that the occurrence of this earthquake is effected by crust fluids. The fluids are thought to result from the dehydration reaction of the subducting slab or the long-term infiltration of the surface water, and the existence of fluids may have enhanced stress concentration in the seismogenic layer leading to mechanical failure, and so can trigger the Kobe earthquake.

When Zhao et al.[29] studied the generating mechanism of western Tottori earthquake occurred in western Japan, they found that the western Tottori mainshock hypocenter is located in a boundary zone where both velocity and Poisson's ratio change drastically. Both P- and S-wave velocities are low in the lower crust under the mainshock hypocenter. They explained that the strong crustal heterogeneities in the western Tottori source area are associated with fluids and arc magma under a nearby volcano. We have obtained similar results in the Landers mainshock hypocenter area. The hypocenter of the Landers earthquake is located in a boundary zone where both velocity and Poisson's ratio change drastically and leans to high Poisson's ratio, and a large low P-wave velocity anomaly is visible under the source zone (Fig. 8). Based on these similar characters, we infer that fluids may also exist in the Landers earthquake area. But a recent study[33] found that there is no slab existing beneath the Southern California, so we infer that the fluids may result from long-term infiltration of surface water, or the surface water infiltrated along the fault zone which was ruptured during the occurrence of last earthquake.

The hypocenter of the Joshua Tree earthquake is located in high P-wave, low S-wave velocity and high Poisson's ratio zone, which is similar to the Bhuj earthquake ($M_{\rm w}$ 7.6) which occurred on January 26, 2001[34]. The mainshock is located in a distinctive zone characterized by high P-wave, low S-wave velocity and high Poisson's ratio. S-wave velocity is more sensitive than P-wave to the fluids, so the S-wave velocity decreases more rapidly. So they inferred that the occurrence of Bhuj earthquake was associated with the influence of fluids. From these results, we can conclude that fluids in the Landers earthquake area play an important role in the occurrence of these large earthquakes.

The hypocenter of Big Bear earthquake ($M_{\rm w}$ 6.5) is located at a distinct zone characterized by high S-wave velocity, low P-wave velocity and low Poisson's ratio. When Nakajima et al.[35] studied the crustal magma and fluids under the volcano area in northeast Japan, they found that the low seismic velocity and low Poisson's ratio anomalies may be caused by fluids (H_2O). We also obtain the similar characters. But we can see that most of the earthquakes occurred above 15 km depth, so the tomographic result is less reliable in the lower crust. More detailed studies are needed to clarify the occurrence mechanism of Big Bear and Joshua Tree earthquakes, such as adding more later phases (e.g. PmP, SmS, sPmP) to the first arrival times to improve tomographic images[36].

Our results indicate that the generation and distribution of earthquakes are different in different regions,

but generation of a large earthquake is closely related to the tectonic environment (such as subduction, active faults, etc.) and physical and chemical properties of materials in the crust and upper mantle (such as magma, fluids, etc.)[29]. The velocity heterogeneities in the middle and lower crust and crustal fluids are important factors for the generation of earthquakes.

6 CONCLUSION

Three-dimensional P- and S-wave velocity and Poisson's ratio structures in Landers epicentral area are determined by using a large number of high-quality arrival times. Main findings about generation and distribution of earthquakes in the Landers earthquake region are summarized as follows.

(1) From the distribution of aftershocks and earthquakes with magnitude larger than 4.0, we can see that velocity heterogeneities are closely related to the distribution of earthquakes. The distribution of the Landers aftershocks is cluster-like and separated or terminated in the area where low-V anomalies exist. Most of the large earthquakes with magnitudes bigger than 4 occur in or around areas with high P-wave velocity. These results possibly indicate that high-velocity areas are probably brittle and strong parts which can sustain seismogenic stress, and so can generate earthquakes. In contrast, low-V areas may have either higher degree of fracture, high fluid pressure, or higher temperatures where deformation is more likely to be aseismic.

(2) Our results show that large earthquakes do not strike anywhere, but are closely related to the tectonic environment. The hypocenter of the Landers earthquake is located in a boundary zone where both velocity and Poisson's ratio change drastically and a large low P-wave velocity anomaly is visible under the source zone which is considered to be associated with fluids. The existence of fluids may weaken the surrounding crustal rocks, which may trigger strong earthquakes.

ACKNOWLEDGMENTS

This work was partially supported by National Natural Science Foundations of China (40434009, 40674048, 40504005) and Japan Society for the Promotion of Science to D. Zhao (Kiban-B No. 11440134, Kiban-A 17204037). We thank Dr. Tian Xiaobo for his thoughtful discussion and suggestions. All the figures are made by using GMT[37].

REFERENCES

[1] Zhao D, Kanamori H, Humphreys E. Simultaneous inversion of local and teleseismic data for the crust and mantle structure of southern California. *Phys. Earth Planet. Inter.*, 1996, **93**: 191∼214

[2] Teng J W. The exchange of substance and energy,different sphere coupling and deep dynamical process within the earth. *Earth Science Frontiers*, 2001, **8**(3): 1∼8

[3] Sieh K, Jones E, Hauksson E, et al. Near-field investigations of the Landers earthquake sequence April to July 1992. *Science*, 1993, **260**: 171∼176

[4] Zhao D, Kanamori H. The 1992 Landers earthquake sequence: earthquake occurrence and structural heterogeneities. *Geophys. Res. Lett.*, 1992, **19**: 1∼4

[5] Liu F T, Li Q, Wu H, et al. Tomographical method used to image reconstruction. *Chinese J. Geophys.* (in Chinese), 1989, **32**(1): 46∼61

[6] Zhao W J, Xue G Q, Wu S H, et al. Fine velocity structure of the upper mantle beneath thee XiZang Plateau from tomography and its geological interpretations. *Chinese J. Geophys.* (in Chinese), 2004, **47**(3): 449∼455

[7] Pei S P, Xu Z H, Wang S Y, et al. Pn velocity tomography of Xinjiang, China and adjacent region. *Chinese J. Geophys.* (in Chinese), 2002, **45**(2): 218∼225

[8] Liu J S, Liu F T, Liu J, et al. Parallel LSQR algorithms used in seismic tomography. *Chinese J. Geophys.* (in Chinese), 2006, **49**(2): 540∼545

[9] Wang F Y, Zhang X K, Chen Q F, et al. Fine tomographic inversion of the upper crust 3D structure around Beijing. *Chinese J. Geophys.* (in Chinese) 2005, **48**(2): 359∼366

[10] Zhao D, Hasegawa A, Horiuchi S. Tomographic imaging of P and S wave velocity structure beneath Northeastern Japan. *J. Geophys. Res.*, 1992, **97**: 19909∼19928

[11] Zhao D, Hasegawa A, Kanamori H. Deep structure of Japan subduction zone as derived from local, regional and teleseismic events. *J. Geophys. Res.*, 1994, **99**: 22313∼22329
[12] Um J, Thurber C. A fast algorithm for two-point seismic ray tracing. *Bull. Seism. Soc. Am.*, 1987, **77**: 972∼986
[13] Paige C, Saunders M. LSQR: An algorithm for sparse linear equations and sparse least squares. *Assoc. Comput. Mach Trans. Math. Software*, 1982, **8**: 43∼71
[14] Christensen N. Poisson's ratio and crustal seismology. *J. Geophys. Res.*, 1996, **101**: 3139∼3156
[15] Zhao D, Kanamori H, Negishi H. Tomography of the source area of the 1995 Kobe earthquake: evidence for fluids at the hypocenter? *Science*, 1996, **274**: 1891∼1894
[16] Zhao D, Ochi F, Hasegawa A, Yamamoto A. Evidence for the location and cause of large crustal earthquakes in Japan. *J. Geophys. Res.*, 2000, **105**: 13579∼13594
[17] Zhao D, Mishra O, Sanda R. Influence of fluids and magma on earthquakes: seismological evidence. *Phys. Earth Planet. Inter.*, 2002, **132**: 249∼267
[18] Humphreys E, Clayton R. Adaptation of back projection tomography to seismic travel time problems. *J. Geophys. Res.*, 1988, **93**: 1073∼1085
[19] Huang J L, Zhao D P, Zheng S H. Seismic tomography of the Sichuan-Yunnan active tectonic region. *Chinese J. Geophys.* (in Chinese), 2001, **44**: 127∼135
[20] Eberhart-Phillips D. Three-dimensional velocity structure in Northern California coast ranges from inversion of local earthquake arrival times. *Bull. Seismol. Soc. Am.*, 1986, **76**(4): 1025∼1052
[21] Kanamori H, Hadley D. Crustal structure and temporal velocity change in Southern California. *Pure and Appl. Geophys.*, 1975, **113**: 257∼280
[22] Lees J, Malin P. Tomographic images of P-wave velocity variations at Parkfield, California. *J. Geophys. Res.*, 1990, **95**: 21793∼21804
[23] Michade A, Eberhart-Plillips D. Relations among fault behavior, subsurface geology, and three-dimensional velocity models. *Science*, 1991, **253**: 651∼654
[24] Teng J W, Zhang B M, Hu J F, et al. The research of deep medium and structural environment of earthquake "pregnancy". In: Chen Y T ed. Advances in Seismology in China: In Honour of Professor Xie Yushou's 80th Birthday. Beijing: Seismological Press, 1997. 258∼265
[25] Sun R M, Liu F T. Crust structure and strong earthquake in Beijing, Tianjin, Tangshan area: I. P wave velocity structure. *Chinese J. Geophys.* (in Chinese), 1995, **38**(5): 651∼654
[26] Sun R M, Zhao Y L, Wu D. Crust structure and strong earthquake in Beijing, Tianjin, Tangshan area: II.S wave velocity structure. *Chinese J. Geophys.* (in Chinese), 1996, **39**(3): 385∼393
[27] Huang J, Zhao D. Crustal heterogeneity and seismotectonics of the region around Beijing, China. *Tectonophysics*, 2004, **385**: 159∼180
[28] Sun R, Liu F, He J, et al. Structural setting of strong earthquakes in the Huabei area of China. *Pure Appl. Geophys.*, 2001, **158**: 903∼918
[29] Zhao D, Tani H, Mishra O. Crustal heterogeneity in the 2000 western Tottori earthquake region: effect of fluids from slab dehydration. *Phys. Earth Planet. Inter.*, 2004, **145**: 161∼177
[30] Johnson P, McEvilly T. Parkfield seismicity: Fluid-driven? *J. Geophys. Res.*, 1995, **100**: 12937∼12950
[31] Xu Ch F. The cause of formation of the upper mantle and crust high conductive layers in Chinese mainland and the study of Tangshan earthquake. *Earth Science Frontiers*, 2003, **10**: 101∼111
[32] Hickman S, Sibson R, Bruhn R. Introduction to special section: Mechanical involvement of fluids in faulting. *J. Geophys. Res.*, 1995, **100**: 12831∼12840
[33] Tian Y, Zhao D, Teng J. Deep structure of Southern California. *Phys. Earth Planet. Inter.*, 2007, **165**(1-2): 93∼113
[34] Kayal J, Zhao D, Mishra O, et al. The 2001 Bhuj earthquake: Tomographic evidence for fluids at the hypocenter and its implications for rupture nucleation. *Geophys. Res. Lett.*, 2002, **29**(24): 2152∼2155
[35] Nakajima J, Matsuzawa T, Hasegawa A, Zhao D. Seismic imaging of arc magma and fluids under the central part of northeastern Japan. *Tectonophysics*, 2001, **341**: 1∼17
[36] Zhao D, Todo S, Lei J. Local earthquake reflection tomography of the Landers aftershock area. *Earth Planet. Sci. Lett.*, 2005, **235**: 623∼631
[37] WESSEL P, SMITH W. New, improved version of the generic mapping tools released. *EOS*, 1998, **79**: 579